SUSTAINED SPATIAL PATTERNS OF ACTIVITY IN NEURONAL POPULATIONS WITHOUT RECURRENT EXCITATION[*]

JONATHAN E. RUBIN[†] AND WILLIAM C. TROY[†]

Abstract. Spatial patterns of neuronal activity arise in a variety of experimental studies. Previous theoretical work has demonstrated that a synaptic architecture featuring recurrent excitation and long-range inhibition can support sustained, spatially patterned solutions in integrodifferential equation models for activity in neuronal populations. However, this architecture is absent in some areas of the brain where persistent activity patterns are observed. Here we show that sustained, spatially localized activity patterns, or bumps, can exist and be linearly stable in neuronal population models without recurrent excitation. These models support at most one bump for each background input level, in contrast to the pairs of bumps found with recurrent excitation. We explore the shape of this bump as well as the mechanisms by which this bump is born and destroyed as background input level changes. Further, we introduce spatial inhomogeneity in coupling and show that this induces bump pinning: for a given starting position, bumps can exist only for a small, discrete set of background input levels, each with a unique corresponding bump width.

Key words. neuronal population, spatial pattern, localized activity bump, off-center coupling, bifurcation, spatial inhomogeneity

AMS subject classifications. 34B15, 34C11, 34C23, 34C37, 93C15

DOI. 10.1137/S0036139903425806

1. Introduction. Evidence suggests that sustained, spatially patterned neuronal activity may play a role in short-term encoding of information. For example, localized persistent activity, or bumps, may provide the basis for a working memory of external stimulus features [14, 7, 18] or a representation of internal states such as head direction (reviewed in [25, 21]). Previous theoretical works have explored the ways in which a network of spiking neurons with short-range recurrent excitation (i.e., positive local coupling) and long-range inhibition can support sustained, spatially organized activity [28, 1, 15, 13, 8, 17, 16, 4, 5]. These studies focus on various forms of rate or activity models, in which a single equation encapsulates the temporal evolution of some measure of the activity level of an entire population of spiking neurons (i.e., neurons firing regularly with some average spike rate). A related result shows that when timescales of synaptic dynamics are taken into account in a conductance-based network model, sustained, localized activity can arise in a two-layer network of *bursting* thalamic cells that lacks recurrent excitation [20]. This leads naturally to the fundamental question of just how crucial the presence of recurrent excitation is for the existence of sustained spatial patterns of activity in rate or activity models of populations of *spiking* neurons. This paper shows that spatially localized activity can be sustained in a neuronal network without recurrent excitation or bursting mechanisms.

We consider a rate model of the form

$$(1.1) \qquad \frac{\partial u(x,t)}{\partial t} = -\sigma u(x,t) + \int_{-\infty}^{\infty} w(x-y)f(u(y,t))\, dy + h.$$
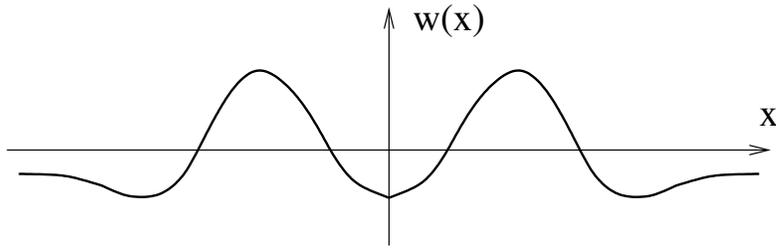
FIG. 1. *Off-center coupling function for an excitatory population. Cells at any position x with $w(x) > 0$ receive excitatory input from cells at position $x = 0$, while cells at x with $w(x) < 0$ receive inhibitory input.*

Equation (1.1) models a single population of spiking neurons. The function $u(x, t)$ encodes the activity level, or average voltage, of a neuronal subgroup at position $x \in (-\infty, \infty)$ and time $t \geq 0$. The connection function $w(x)$ determines the coupling between subgroups, and the nonnegative, nondecreasing function $f(u)$ denotes the neuronal firing rate, or average rate at which spikes are generated, corresponding to an activity level u. Neurons at a point x are said to be active if $f(u(x,t)) > 0$. Finally, the parameter h encodes a constant external stimulus applied uniformly to the entire neural field [1], such as an average background input level received from other areas of the brain, and the parameter σ denotes a positive rate constant; the ratio h/σ represents the baseline level of activity in the population without coupling. Without loss of generality, we set $\sigma = 1$.

In this paper, we take $f(u(x,t)) = H(u(x,t))$, the Heaviside step function, which gives

$$(1.2) \qquad \frac{\partial u(x,t)}{\partial t} = -u(x,t) + \int_{-\infty}^{\infty} w(x-y) H(u(y,t)) \, dy + h.$$

For the Heaviside form of firing rate function, the activity level $u = 0$ represents an absolute threshold for synaptic input required to drive spiking activity. This form of (1.1) was considered in [1] and by many subsequent authors. Further, it was shown in [15] that results for (1.2) are crucial in determining solution structure for (1.1) with more general nondecreasing f.

After we detail additional assumptions on the model, we prove that recurrent excitation is not necessary for the existence of stable stationary, spatially localized solutions (i.e., bumps) in populations of spiking cells. The synaptic architecture that we consider, as an alternative to recurrent excitation, takes the form shown in Figure 1. Such an *off-center architecture* may be relevant in several different contexts. For example, consider a network featuring interconnected excitatory (E) and inhibitory (I) populations of cells, in which E-cells are intrinsically capable of spiking and I-cells inhibit both E-cells and other I-cells. In such a network, activity of E-cells leads to activity of corresponding I-cells. This may lead to feedback inhibition onto the active E-cells as well as inhibition of nearby I-cells. This I-I inhibition can in turn disinhibit nearby E-cells, effectively acting as an off-center form of excitation onto E-cells, as portrayed in Figure 1. This form of architecture may arise in interactions of the subthalamic nucleus (E) and external segment of the globus pallidus (I) in the primate basal ganglia [22, 26]. It also may occur in interactions of thalamocortical

relay cells (E) and thalamic reticular cells (I) in the thalamus in awake states, where activity bumps in certain subpopulations of cells can encode head direction [23, 24]. Long-range inhibitory connections have been found in the thalamus [9, 10], but no thalamic recurrent excitatory connections are known to exist. In the first subsection of the appendix, we discuss the derivation of the effective coupling shown in Figure 1 from coupled E and I populations modelled by a pair of equations of the form (1.1), as in [28, 1, 19] but without recurrent excitation, although a rigorous mathematical derivation, or a complete mathematical treatment of the coupled equations, remains for future research. Alternatively, this form of suppression of recurrent excitation by localized inhibitory feedback may be generated by inhibitory interneurons in a variety of cortical areas, or in the CA1 region of the hippocampus, which features at most sparse recurrent excitatory connections [6, 27].

We consider this coupling architecture in section 2. Under certain assumptions, we prove the existence of a bump solution $u(x)$ to (1.2) such that $u(x) > 0$ if and only if $x \in (0, a)$ for a fixed constant a. We also show that this bump solution is linearly stable when it exists. Our proof method for existence generalizes that given by Amari [1] for bumps in (1.2) with lateral inhibition. However, details become much more subtle due to the more complicated synaptic architecture that we consider.

Unlike the case with recurrent excitation, where two bump solutions exist [1], the bump of localized positive activity that we find is unique for each fixed h in some finite interval. We show how the shape of a bump depends on its size, which in turn depends on h, relative to certain features of the coupling function $w(x)$. Further, as h varies, bump solutions (parametrized by h) are created and destroyed by atypical mechanisms that do not involve saddle-node bifurcations (since only a single solution exists for each h) or the entire bump collapsing to 0, and we explain the possible mechanisms and how they are selected.

For consideration of stability, we deviate from [1] to give a rigorous linear stability calculation. A simplified version of the calculation shows that a spatially uniform state can also be stable, such that the system exhibits bistability, consistent with [20, 24].

It has been argued that coupling strengths between neurons should not be purely distance dependent but rather should allow for spatial variation [2, 3]. In section 3, we introduce spatial inhomogeneity in coupling, replacing $w(x-y)$ by $w(x-y)p(y)$ under the integral in equation (1.2). We set up equations relevant to bump existence in this case, which we treat through a combination of analysis and numerics. The presence of spatial inhomogeneity naturally destroys the translation invariance of bumps. In fact, we find that it induces a form of bump pinning, such that for a given starting position, bumps exist for only a small, discrete set of background input levels, each with a unique corresponding bump width. Interestingly, in our primary numerical example, we find that there is a special bump width which is possible for any starting position. We comment on possible functional implications of these results in the discussion in section 4.

2. Spatially homogeneous coupling.

2.1. Assumptions. In this section, we consider (1.2)

$$\frac{\partial u(x,t)}{\partial t} = -u(x,t) + \int_{-\infty}^{\infty} w(x-y)H(u(y,t))\,dy + h$$

with a coupling function $w(x)$ satisfying the hypothesis

(H1) $w(x)$ is continuous and integrable on $\mathbb{R}$ and is symmetric; i.e., $w(-x) = w(x)$ for all $x \in \mathbb{R}$.

Moreover, we assume that there exist constants $x_* > x_1 > x^* > x_0 > 0$ such that

$(H2)$ $w(x) < 0$ on $(-x_0, x_0)$ and on (x_1, ∞), with $w(x_0) = w(x_1) = 0$;

$(H3)$ $w(x)$ is increasing on $(0, x^*)$ and on (x_*, ∞);

$(H4)$ $w(x) > 0$ on (x_0, x_1);

$(H5)$ $w(x)$ is decreasing on (x^*, x_*).

Coupling functions that satisfy $(H2)$ and $(H4)$ are sometimes called off-center coupling functions.

To simplify notation, we will also assume the following symmetry hypothesis in certain cases noted below

$(H6)$ there exists $\delta > 0$ such that $x_1 = x^* + \delta$ and $x_0 = x^* - \delta$, and $w(x^* + \eta) = w(x^* - \eta)$ for all $\eta \in [0, \delta]$.

We will comment further on the role of this hypothesis in Remark 2.8 after the proof of Theorem 2.5. A coupling function $w(x)$ satisfying $(H1)$–$(H6)$ appears in Figure 2.
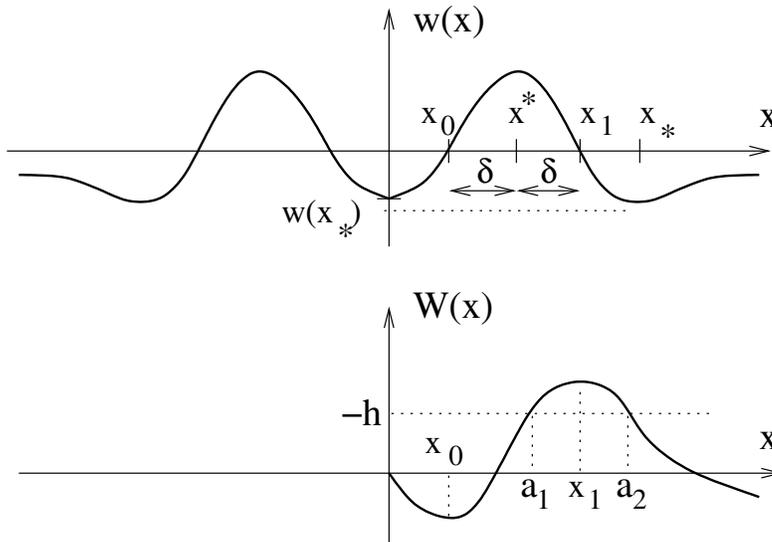

FIG. 2. *Off-center coupling function $w(x)$, together with antiderivative $W(x)$. From the plot of $W(x)$, we can visualize the necessary condition (2.3), $W(a) + h = 0$, for bump existence.*

2.2. Existence of a unique bump. Following Amari [1], we seek stationary bump solutions $u(x)$ to (1.2), for which $u(x) > 0$ if and only if $x \in (0, a)$ for some constant a. Note that this is equivalent to the existence of a bump on any other interval of length a; that is, the system is translation invariant. Such solutions satisfy the condition

$$(2.1) \qquad u(x) = \int_0^a w(x - y)\, dy + h\,.$$

Since $\lim_{x \to \infty} w(x) = 0$, the fact that $\lim_{x \to \infty} u(x) \le 0$ for such a solution requires that $h \le 0$. Thus, we impose the existence condition that

$(E1)$ the constant $h \le 0$.

Let $W(x) = \int_0^x w(t)\,dt$, which is an odd function. Then (2.1) becomes

$$(2.2) \qquad u(x) = W(x) - W(x - a) + h.$$

From (2.2), the conditions $u(0) = 0$ and $u(a) = 0$ both give

$$(2.3) \qquad W(a) + h = 0.$$

Figure 2 displays a graphical representation of equation (2.3). Note that for fixed $h < 0$, there exist either zero or two solutions of (2.1), unless $-h = W(x_1)$.

We will require a second existence condition, namely, that

(E2) $W(x) + h > 0$ for some $x \in \mathbb{R}^+$ and $\lim_{x \to \infty} W(x) < -h$.

For fixed h such that conditions (E1) and (E2) hold, there exist two nonzero solutions of (2.3). We label these solutions as a_1 and a_2, where $a_2 > x_1 > a_1 > 0$. Note that a_2 could fail to exist without (E2), if $\lim_{x \to \infty} W(x) > -h > 0$. Let $u_1(x), u_2(x)$ denote the corresponding functions defined by $u_i(x) = W(x) - W(x - a_i) + h$. Note that $u_i(x) = W(x) - W(x - a_i) + h = W(a_i - x) + W(x) + h = u(a_i - x)$ for all x. This yields the following symmetry statement.

PROPOSITION 2.1. *Each solution $u_i(x)$ of (2.3) is symmetric about $x = a_i/2$.*

With these definitions, we state one final hypothesis, as an alternative to (H6), that will be assumed when noted below:

(H6′) $W(x_0) - W(a_2) + W(a_2 - a_1) > 0$.

PROPOSITION 2.2. *Assume (H1)–(H5). Fix h such that (E1)–(E2) hold and $a_1 < x_1$ such that $W(a_1) + h = 0$. The function $u_1(x)$ defined by (2.1) with $a = a_1$ does not represent a valid bump solution to (1.2). In fact, if we assume (H6) as well, then $u_1(x) < 0$ on all of $(0, a_1)$.*

Proof. By construction, $u_1(0) = 0$ and $x_0 < a_1 < x_1$. Note that $u_1'(x) = w(x) - w(a_1 - x)$. Since $a_1 < x_1$, it follows that $w(a_1) > w(0)$. Thus, $u_1'(0) = w(0) - w(a_1) < 0$. This establishes that $u_1(x)$ is not a valid bump.

Further, note that $u_1'(x) = 0$ requires $w(x) = w(a_1 - x)$. This occurs at $x = a_1/2$, consistent with the symmetry of $u_1(x)$ about $x = a_1/2$. However, we shall see that when (H6) holds, the equation $u_1'(x) = 0$ has no other solutions in $(0, a_1)$, proving the proposition. To see this, note that by (H6), if there exists $x \neq a_1/2$ in $(0, a_1)$ such that $u_1'(x) = 0$, then $(a_1 - x) - x^* = x^* - x$, or, equivalently, $a_1 = 2x^*$. But $a_1 < x_1 < x_1 + x_0 = 2x^*$, so this is not possible. $\square$

Remark 2.3. Proposition 2.2 implies that a bump can only possibly exist when there exists $a_2 > x_1$ for which (2.3) holds. Thus, if $\lim_{x \to \infty} W(x) > -h$, in violation of (E2), then no bump exists.

Now, define the constant A as the smallest positive x value for which $W(x) = 0$, guaranteed to exist by (E2) since $h \leq 0$.

PROPOSITION 2.4. *Assume (H1)–(H5). Fix h such that (E1)–(E2) hold. If $0 < a_2 - a_1 < A$, then the function $u_2(x)$, defined by (2.1) with $a = a_2$, does not represent a valid bump solution to (1.2).*

Proof. We compute directly from equation (2.2) that

$$u_2(a_1) = W(a_1) + W(a_2 - a_1) - W(a_1) = W(a_2 - a_1).$$

If $a_2 - a_1 < A$, then $u_2(a_1) < 0$. But $a_1 \in (0, a_2)$, so $u_2(x)$ is not a bump. $\square$

Next we establish some results showing the existence of a valid bump in various cases. Note that if $\lim_{x \to \infty} W(x) = 0$ (see Figure 2), then we can make a_2 arbitrarily large by choosing h sufficiently close to 0. If $a_2/2 > x_1$, then $a_2 - a_1 > 2x_1 - a_1 >$

$a_1 > A$. Thus, when $a_2/2 > x_1$, Proposition 2.4 does not apply, and $u_2(a_1) > 0$. In fact, in this case, we can establish the existence of a bump without hypothesis $(H6)$ or $(H6')$, as addressed below in Theorem 2.5. However, as we shall see in subsection 2.4, a_2 can also become too large for a bump to exist. This motivates a final existence condition,

$(E3)$ $w(a_2 \pm x_0) < w(0)$.

As we make h more negative, such that $-h$ grows toward the peak of W, we will also need to impose $(H6)$ or $(H6')$ to ensure the existence of a bump.

THEOREM 2.5. *Assume that $(H1)$–$(H5)$ hold. Fix h such that $(E1)$–$(E3)$ hold and assume that $a_2/2 > x_1$. Then the function $u_2(x)$ defined by (2.1) with $a = a_2$, such that $-W(a_2) = h$, is a bump solution to (1.2), with $u_2(x) > 0$ if and only if $x \in (0, a_2)$.*

Proof. First, recall that $a_2 > x_1$, since $W(a_2) = -h > 0$ and $W'(a_2) = w(a_2) < 0$ (see Figure 2). Further, since $w(0) < 0$ and $w(x_1) = 0$, the hypotheses of the theorem together with $(H2)$–$(H5)$ imply that there exist exactly two positive values $x'' > x' > x_1$ such that $w(0) = w(x') = w(x'')$, and $a_2 \in (x' + x_0, x'' - x_0)$; see Figure 3. This gives $w(0) > w(a_2)$ and $a_2/2 > x_0$.

We now show that $u_2(x) > 0$ for $x \in (0, a_2)$. First, we consider $x \in (0, x_0]$. Note that

$$(2.4) \qquad\qquad u_2'(x) = w(x) - w(a_2 - x)$$

from (2.2). In particular, $u_2'(0) = w(0) - w(a_2) > 0$. Since $a_2 > x' + x_0$, we have $a_2 - x > x'$ for all $x \in (0, x_0]$. Thus, $w(a_2 - x) < w(x)$ and $u_2'(x) > 0$ for all $x \in (0, x_0]$.

Next, suppose that $a_2/2 > x_1$. Now, $u_2'(x) = w(x) - w(a_2 - x) > 0$ on $(x_0, x_1]$ as well. This holds because on $(x_0, x_1]$, $w(x) \geq 0$, while $a_2 - x > a_2 - x_1 > x_1$, such that $w(a_2 - x) < 0$ by $(H2)$. It remains to show that $u_2(x) > 0$ for all $x \in (x_1, a_2)$. To do this, it suffices to show that $u_2(x) > 0$ for all $x \in (x_1, a_2/2]$, since symmetry (Proposition 2.1) then gives $u_2(x) > 0$ for all $x \in (0, a_2)$.

Equation (2.2) can be rewritten for $u = u_2(x)$ as

$$(2.5) \qquad\qquad u_2(x) = (W(x) - W(a_2)) + W(a_2 - x),$$

using equation (2.3) and the fact that $W(x)$ is odd. We will show that $u_2(x)$ in (2.5) is the sum of two positive terms for $x \in (x_1, a_2/2]$. When $x_1 < x \leq a_2/2$, it follows that $a_2 - x_1 > a_2 - x \geq a_2/2 > x_1$. By construction, $W(x) > 0$ on $[x_1, a_2]$. Hence, $W(a_2 - x) > 0$ for all $x \in (x_1, a_2/2]$. Now, consider the first term in $u_2(x)$ in (2.5), namely, $W(x) - W(a_2)$, for $x \in (x_1, a_2/2]$. Since $W'(x) = w(x) < 0$ on (x_1, ∞) by $(H2)$, and $x_1 < x \leq a_2/2 < a_2$, we have $W(x) > W(a_2)$ for all $x \in (x_1, a_2/2]$. Thus, $u_2(x)$ is the sum of two positive terms, and hence is positive, on $(x_1, a_2/2]$, as claimed. This gives $u_2(x) > 0$ on $(0, a_2)$, as desired.

Finally, to complete the proof, we confirm that $u_2(x) < 0$ for all $x \in (a_2, \infty)$. Note that since $W(a_2) = -h > 0$, $u_2(x) < 0$ is equivalent to $W(x) < W(a_2) + W(x - a_2)$ by equation (2.3). Since $W(a_2) > 0$, we have $u_2(x) < 0$ for all x such that $W(x - a_2) \geq W(x)$. Since $W(x)$ decreases on (x_1, ∞), this implies that $u_2(x) < 0$ for $x - a_2 \geq x_1$, namely, $x \in [a_2 + x_1, \infty)$. Thus, it remains to consider $x \in (a_2, a_2 + x_1)$. We will show that $u_2'(x) < 0$ on $(a_2, a_2 + x_1)$, for $u_2'(x)$ given in (2.4), such that $u_2(x)$ remains negative there. Since $w(x - a_2) > 0$ on $(a_2 + x_0, a_2 + x_1)$ by $(H4)$, while $w(x) < 0$ on this interval by $(H2)$, it is obvious from (2.4) that $u_2'(x) < 0$ on $(a_2 + x_0, a_2 + x_1)$. It remains only to consider $x \in (a_2, a_2 + x_0]$. Condition $(E3)$ gives $w(a_2) < w(0)$, so
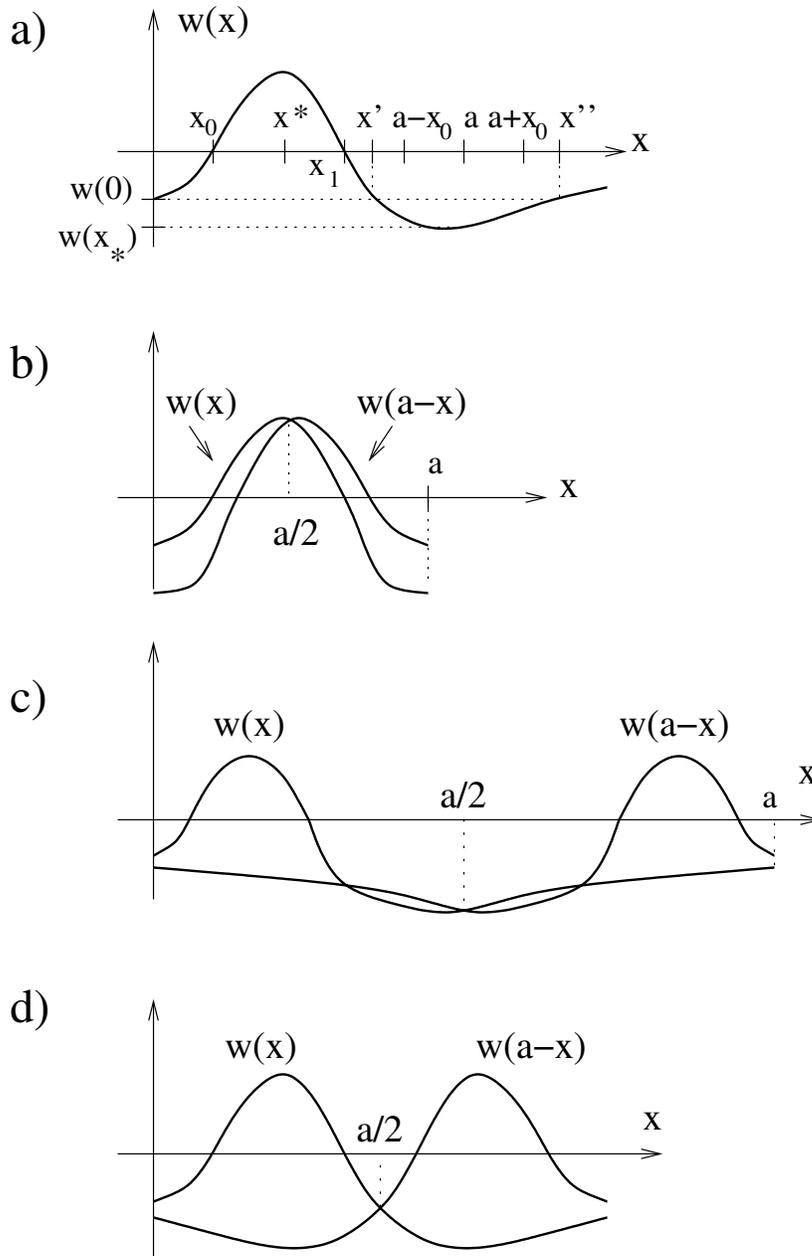
FIG. 3. *Graphical representation of Theorems* 2.5, 2.7, 2.9, *and* 2.13. *Here,* a *denotes* a_2 *from the theorems.* (a) *Illustration of the hypotheses of the theorems.* (b) *The relation of* $w(x), w(a_2 - x)$ *resulting from the proof of Theorem* 2.9, *if* $a_2/2 \leq x_1$. (c) *The relation of* $w(x), w(a_2 - x)$ *shown in Theorem* 2.13 *if* $a_2/2 \in (x_1, x_*]$. (d) *The relation of* $w(x), w(a_2 - x)$ *shown in Theorem* 2.13 *if* $a_2/2 > x_*$.

$u_2'(a_2) < 0$. For $x \in (a_2, a_2+x_0]$, we have $w(x) < w(0)$ by $(E3)$, while $w(x-a_2) > w(0)$ by $(H3)$. Thus, $u_2'(x)$ remains negative, as desired. □

Theorem 2.5 establishes the existence of a bump $u_2(x)$ when $a_2/2 > x_1$. Next, we consider the case of $a_2/2 \le x_1$, corresponding to more negative choices of h. In this situation, we will prove two different theorems that invoke $(H6')$ and $(H6)$, respectively. Note that it is natural to interpret $(H6')$ as an assumption on the value of h, for fixed w. On the other hand, $(H6)$ is an assumption about the shape of w, independent of h. When we assume $(H6)$ below, we restrict the class of w considered, and we correspondingly restrict the shape of the bump produced (see Theorem 2.9).

Remark 2.6. Note that the proof that $u_2(x) < 0$ for all $x \in (a_2, \infty)$ does not require $a_2/2 > x_1$. Thus, in the proofs of Theorems 2.7 and 2.9 below, we will not repeat the corresponding arguments.

THEOREM 2.7. *Assume that w and h are chosen such that $(H1)$–$(H5)$, $(E1)$– $(E3)$, and $(H6')$ hold and such that $a_2/2 \le x_1$. Then the function $u_2(x)$ defined by (2.1) with $a = a_2$, such that $-W(a_2) = h$, is a bump solution to (1.2), with $u_2(x) > 0$ if and only if $x \in (0, a_2)$.*

Proof. By symmetry (Proposition 2.1), it suffices to show that $u_2(x) > 0$ on $(0, a_2/2]$. From the proof of Theorem 2.5, we already have $u_2'(x) > 0$ on $(0, x_0]$. We will first consider $x \in (a_1, a_2/2]$ and then $x \in (x_0, a_1]$. Note that by $(H6')$, $W(a_2 - a_1) > W(a_2)$, so $a_2 - a_1 > a_1$, and thus the interval $(a_1, a_2/2]$ is nonempty. For $x \in (a_1, a_2/2]$, we have $a_2 - x \in (a_1, a_2)$, since

$$a_1 < x < a_2/2 \le a_2 - x < a_2.$$

Thus, $W(a_2 - x) > -h > 0$, with a similar inequality for $W(x)$. Equation (2.2), together with the fact that W is odd, therefore gives

$$u(x) = W(x) + W(a_2 - x) + h > W(a_2 - x) > -h > 0$$

for $x \in (a_1, a_2/2]$.

Next, suppose $x \in (x_0, a_1]$. Note that over the range of positive x-values, the minimum value of W occurs at $x = x_0$, so

$$(2.6) \qquad u(x) > W(x_0) + W(a_2 - x) + h =: F(x) \quad \text{for } x \in (x_0, a_1].$$

$F(x_0) = u(x_0)$ by comparison of (2.2) and (2.6), and $u'(x) > 0$ on $(0, x_0]$ gives $u(x_0) > 0$, so $F(x_0) > 0$. Next, note that $F'(x) = -w(a_2 - x)$, so since $w(a_2 - x_0) < w(0) < 0$, it follows that $F'(x_0) > 0$.

Suppose that for some $x_f \in (x_0, a_1]$, $F'(x_f) = 0$. Then $w(a_2 - x_f) = 0$, so either $a_2 - x_f = x_0$ or $a_2 - x_f = x_1$ (see Figure 2). In the former case, we would have $x_f = a_2 - x_0 > x_1 > a_1$, however, so this cannot occur, and $a_2 - x_f = x_1$. Thus, $F''(x_f) = w'(a_2 - x_f) = w'(x_1) < 0$. Since $F(a_1) > 0$ by $(H6')$, the maximum principle implies that $F > 0$ on the entire interval $[x_0, a_1]$.

In summary, $u(x) > F(x) > 0$ on $(x_0, a_1]$. Thus, the proof is complete. □

Remark 2.8. Note that hypothesis $(H6')$ requires $a_2 - a_1 > A$. That is, if $a_2 - a_1 < A$, then $W(x_0), -W(a_2)$, and $W(a_2 - a_1)$ are all negative terms, and $(H6')$ cannot hold. Thus $(H6')$ ensures that we are in a regime in which Proposition 2.4 does not apply.

To conclude this subsection, we show that under the symmetry hypothesis $(H6)$, there exists a bump $u_2(x)$ that is monotone increasing on $[0, a_2/2)$ and monotone decreasing on $(a_2/2, a_2]$, for $a_2/2 \le x_1$.

THEOREM 2.9. *Assume that $(H1)$–$(H6)$ hold. Fix h such that $(E1)$–$(E3)$ hold and such that $a_2/2 \leq x_1$. Then the function $u_2(x)$ defined by (2.1) with $a = a_2$, such that $-W(a_2) = h$, is a bump solution to (1.2), with $u_2(x) > 0$ if and only if $x \in (0, a_2)$. Moreover, $u'_2(x) > 0$ on $[0, a_2/2)$ and $u'_2(x) < 0$ on $(a_2/2, a_2]$.*

Proof. Again, from the proof of Theorem 2.5, we have $u'_2(x) > 0$ on $(0, x_0]$. Now, suppose that $a_2/2 \leq x_1$. By the assumption of the theorem, $a_2 - x_0 > x' > x_1$. Therefore, $a_2/2 > (x_0 + x_1)/2 = x^*$. Together with $(H6)$, this implies that $w(a_2 - x) < w(x)$ remains true on $(0, x^*]$, that $w(a_2 - x) = w(x)$ precisely at $x = a_2/2 \in (x^*, a_2 - x^*)$, and $w(a_2 - x) > w(x)$ on $(a_2/2, a_2]$ (see Figures 2 and 3(a) and (b)). Thus, $u_2(x) > 0$ for all $x \in (0, a_2)$, with $u_2(a_2) = 0$, if $a_2/2 \leq x_1$. □

COROLLARY 2.10. *Let $w = w(x, \mu)$ be continuous in $\mu \in \mathbb{R}$ and set $W(x, \mu) = \int_0^x w(t, \mu) \, dt$. Assume that w satisfies $(H1)$–$(H5)$ for all μ in a neighborhood of $\mu = 0$ and that $w(x, 0)$ satisfies $(H6)$. Then there exist $\mu_1 < 0 < \mu_2$ and a function $a(\mu)$, with $a(0) = a_2$ given by $-W(a_2, 0) = h$, such that a bump solution $u_\mu(x)$ of (1.2) exists, with $u_\mu(x) > 0$ if and only if $x \in (0, a(\mu))$, for all $\mu \in (\mu_1, \mu_2)$.*

Proof. By the implicit function theorem, since $W_x(a_2, 0) \neq 0$, a unique function $a(\mu)$ satisfying $W(a(\mu), \mu) + h = 0$ exists near $\mu = 0$, with $a(0) = a_2$. The existence of the bump solution $u_\mu(x)$ then follows immediately from the proof of Theorem 2.5, for $|\mu|$ sufficiently small. □

Remark 2.11. Without hypothesis $(H6)$, or some other restriction on the behavior of $w(x)$, there could be an unlimited variety of zeros of $u'_2(x)$ on $(0, a_2)$, depending on the relative rates of change of w to the left and right of x^*. In fact, without some hypothesis such as $(H6)$ or $(H6')$, $u_2(x)$ could become negative inside $(0, a_2)$, and the bump could fail to exist, as seen in Proposition 2.4. This issue is explored further in subsection 2.4.

Remark 2.12. The condition $(H6)$ as stated may seem to represent somewhat restrictive conditions to be achieved as an architecture of synaptic connections in a biological neuronal network. However, suppose we consider bumps as a form of memory. It is possible that for a given pattern of past experiences, only certain sub-networks within a coupled E-I network should be able to form bumps, corresponding to the particular memories stored in the network. The learning process could consist of the scaling of synaptic connections and their associated weights to develop particular architectural patterns. From this viewpoint, restrictions on synaptic architectures required for the appearance of bumps might be an essential feature of E-I networks, to prevent spurious overactivity. See the discussion in section 4 for consideration of related ideas.

2.3. The shape of the bump without $(H6)$ or $(H6')$. We have already seen that hypothesis $(H6)$ gives certain monotonicity properties for the bump $u_2(x)$ when $a_2/2 \leq x_1$. We next characterize more generally how the shape of $u_2(x)$ depends on the position of a_2, without assuming $(H6)$ or $(H6')$, when $a_2/2 > x_1$.

THEOREM 2.13. *If $a_2/2 \in (x_1, x_*]$, then u_2 has a unique global maximum at $x = a_2/2$. If $a_2/2 > x_*$, then $u'_2(x)$ has at least three zeroes on $(0, a_2)$, including a local minimum of $u_2(x)$ at $x = a_2/2$.*

Proof. Suppose that $a_2/2 > x_1$. We look for zeroes of $u'_2(x)$, as given in equation (2.4). From the proof of Theorem 2.5, we already know that $u'_2(x) > 0$ on $(0, x_0]$. The condition $a_2/2 > x_1$ implies that

$$(2.7) \qquad\qquad w(x_1) = 0 > w(a_2 - x_1),$$

so in fact $w(x) \geq 0 > w(a_2 - x)$ for all $x \in (x_0, x_1]$ and $u_2'(x) > 0$ on $(x_0, x_1]$. Suppose that $a_2/2 \leq x_*$, the point where $w(x)$ has its minimum (see Figure 3(a)), and define $\bar{x}$ by $a_2 - \bar{x} = x_*$. Then $\bar{x} = a_2 - x_* \leq x_*$. Thus, $w(a_2 - x) = w(x)$ at exactly one value $x \in (\bar{x}, x_*]$, namely, at $x = a_2/2$, and this is the only zero of $u_2'(x)$ in $(0, a_2)$. As in the previous case, this is a global maximum for $u_2(x)$ (see Figure 3(d)).

We now show that if $a_2/2 > x_*$, then in fact $u_2'(x) = w(a_2 - x) - w(x)$ has at least *three* zeroes (see Figure 3(c)). To see this, first note that inequality (2.7) still holds, since we still have $a_2/2 > x_1$. However, $w(x_*) < w(a_2 - x_*)$, since $a_2 - x_* > x_*$ and $w(x)$ has its minimum at $x = x_*$. Thus, $u_2'(x)$ has at least one zero on (x_1, x_*). For $x > x_*$, $w(x)$ is increasing by $(H3)$, while $w(a_2 - x)$ decreases until $x = a_2 - x_*$, at which point $w(x) > w(a_2 - x)$. Thus, exactly one additional zero of $u_2'(x)$ occurs on $(x_*, a_2 - x_*)$. Since $a_2/2 > x_*$, we have $a_2 - x_* > a_2/2$. As noted earlier, $u_2'(x)$ has a zero at $x = a_2/2$ from the form of (2.4); hence, this second zero must occur at $x = a_2/2$, and $u_2'(x)$ has at least one more zero for $x > a_2 - x_*$, by symmetry.

From (2.4), it follows that $u_2''(x) = w'(x) + w'(a_2 - x)$, such that $u_2''(a_2/2) = 2w'(a_2/2)$. When $a_2/2 > x_*$, we have $w'(a_2/2) > 0$ by $(H3)$, such that $u_2''(a_2/2) > 0$; that is, u_2 has a local minimum at $a_2/2$, completing the proof. □

Remark 2.14. Examples of bump solutions $u_2(x)$ of (2.1) with $a_2/2 < x_*$ and $a_2/2 > x_*$, respectively, are shown in Figure 4. These plots were generated by solving (2.1) numerically with a coupling function $w(x)$ defined in a piecewise manner on $[0, \infty)$ as

$$(2.8) \qquad w(x) = \begin{cases} -Kx(x-1) - \epsilon, & x \in [0, 1), \\ -(x - 1 + \epsilon)e^{-b(x-1)}, & x \in [1, \infty) \end{cases}$$

for $K, b > 0$ and $0 < \epsilon < \min\{K/4, 1/b\}$, and then extended to be even on $(-\infty, \infty)$. This function satisfies $(H1)$. It also satisfies $(H2)$ and $(H4)$, with $x_0 = \frac{1}{2}[1 - \sqrt{1 - 4\epsilon/K}]$ and $x_1 = \frac{1}{2}[1 + \sqrt{1 - 4\epsilon/K}] < 1$. Assumptions $(H3)$ and $(H5)$ hold for this $w(x)$ as well, with $x^* = 1/2$ and $x_* = 1 + 1/b - \epsilon$. Finally, $w(x)$ is symmetric about $x^* = 1/2$ on (x_0, x_1), satisfying $(H6)$.

From (2.4), no matter what the value of a_2, we have $u_2'(a_2/2) = 0$. Thus, it is of interest to estimate $u_2(a_2/2)$.

PROPOSITION 2.15. *If $a_2/2 > a_1$ and $u_2(x) > 0$ on $(0, a_2)$, then $u_2(a_2/2) > -h$.*

Proof. If $a_2/2 > a_1$, then $a_2/2 \in (a_1, a_2)$, so $W(a_2/2) > -h$ (see Figure 2). From (2.2), this implies

$$u_2(a_2/2) = 2W(a_2/2) + h > W(a_2/2) > -h\,. \qquad □$$

Combining Theorem 2.13 and Proposition 2.15 yields the following result.

COROLLARY 2.16. *If a bump $u_2(x)$ exists with $a_2/2 \in (x_1, x_*]$, then the activity level $u_2(x)$ attains a maximum value greater than $-h$. If a bump $u_2(x)$ exists with $a_2/2 > x_*$, then at the local activity minimum $a_2/2$, the activity level is bounded below by $-h$.*

2.4. Birth and death of bumps. We have seen that the function $u_2(x)$ is a bump for some values of a_2, but may fail to be a bump in some cases, such as $a_2 - a_1 < A$, as in Proposition 2.2. In fact, since $\lim_{x\to\infty} w(x) = 0$, we will see below that the interval of a values on which $u_2(x)$ is a valid bump is finite. Thus, a family of bump solutions, parametrized by bump length a, must be born at some finite value of a and must die at some larger finite value of a. In this subsection,
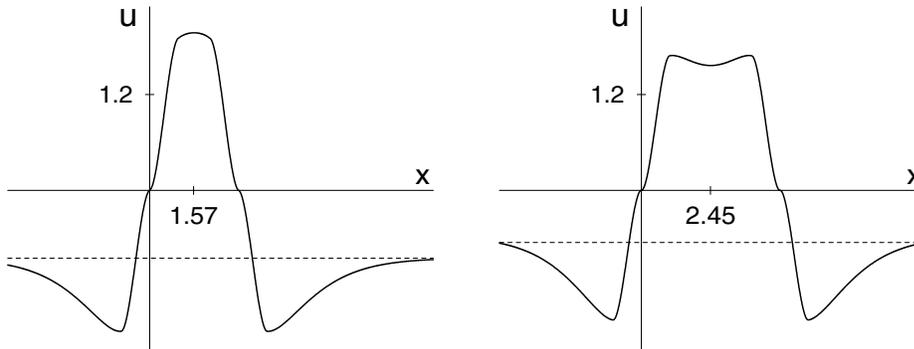
FIG. 4. *Bump solutions of (2.1) for the coupling function $w(x)$ given in (2.8) and extended in an even manner. Parameters used are $K = 10.0, \epsilon = 0.1, b = 1.0$, such that $x_* = 1.9$. Left: A bump with no local minimum, found with $h = -0.85$, such that $a_2 = 3.15 < 2x_*$. Right: A bump with a local minimum at $a_2/2 > x_*$, found with $h = -0.57$, such that $a_2 = 4.90 > 2x_*$. Dashed lines show the levels of h.*

we discuss possible mechanisms by which bumps may be created or destroyed as a varies (which can be achieved by varying h). We shall see that this does not occur through a "usual" bifurcation mechanism, such as a saddle-node bifurcation, and that when bumps arise, they do so with a finite amplitude. This contrasts with the situation when the coupling function $w(x)$ is derived from recurrent excitation and lateral inhibition, in which case bump amplitudes and widths may go to zero as a parameter varies.

In the following analysis, we will always assume $a > x_1$, corresponding to the possible bump solution $u_2(x)$, since $u_1(x)$ is never a valid bump. We will also assume that $W(a) > 0$, also necessary for a to represent a bump length since $h < 0$ in (2.3).

In general, there are two types of transitions through which a bump $u_2(x)$ may cease to exist as its size a varies, even without interaction with any other solutions. One possibility is that a bump may go negative on its interior; that is, it may develop a dip as in Figure 4, which may continue to drop until the minimum value of $u_2(x)$ on $(0, a)$ passes through 0. We refer to this as the *internal tangency* mechanism, since right at the transitional a value, we have $u_2(x) = u_2'(x) = 0$ for some $x \in (0, a)$. By (2.5),

$$(2.9) \qquad\qquad u_2(a/2) = 2W(a/2) - W(a).$$

We will use (2.9) to show that $u_2(a/2) = 0$ can occur only at a unique value of $a > x_1$.

PROPOSITION 2.17. *There is at most one value of $a > x_1$ for which $W(a) > 0$ and $u_2(a/2) = 0$.*

Proof. Suppose $u_2(a_0/2) = 0$ and $W(a_0) > 0$ for $a_0 > x_1$. Then $W(a_0) > 0$ implies that $W(a_0/2) > 0$, by (2.9). Thus, $a_0/2 > A$, where A was defined as the smallest positive value for which $W(x) = 0$. Moreover, $W(a_0) = 2W(a_0/2)$ implies that $W(a_0) > W(a_0/2)$, so $a_0/2 < x_1$ (e.g., Figure 2).

Now, let $z(a) = 2W(a/2) - W(a)$. For $a/2 \in (A, x_1)$, $W'(a/2) > 0$, while $a > x_1$ gives $W'(a) < 0$. Thus, $z'(a) > 0$ and z can have at most one zero with $a/2 \in (A, x_1)$. Since $a_0/2$ must lie in this interval whenever $u_2(a_0/2) = 0$, this concludes the proof. □

Proposition 2.17 rules out the possibility that a family of bump solutions both arises and dies by passage of $u_2(a/2)$ through 0. However, it does not rule out the possibility that the birth and the death of the family are associated with dips on the interior of $(0, a)$ switching from negative to positive and from positive to negative, respectively. Indeed, it is possible that $u_2(a/2 - \delta) = 0$ for some $\delta \in (0, a/2)$, with $u_2(a/2 + \delta) = 0$ as well by Proposition 2.1. Thus, there are infinitely many positions at which interior zeros of u_2 could develop, always occurring in groups of even numbers of dips, placed symmetrically about $a/2$.

An alternative to the internal tangency mechanism for birth and death of bumps is that $u_2'(0)$ (and by symmetry, $u_2'(a)$) may become zero and then negative (positive) as a varies. We refer to this transition as the *boundary tangency* mechanism. Note that $u_2'(0) = w(0) - w(a)$, where a is the length of $u_2(x)$. Thus, $u_2'(0) < 0$ for $a \in (x_1, x')$, and, since $\lim_{x \to \infty} w(x) = 0$, $u_2'(0) < 0$ for all $a > x''$ (see Figure 3). Hence, the boundary tangency mechanism ensures that the family of bumps can exist only on a finite interval of positive a values.

Note further that $u_2''(0) = w'(0) + w'(a) = w'(a)$. If $u_2'(0) = 0$ for some a at which a transition between bump existence and bump nonexistence occurs, then we must have $u_2''(0) > 0$ (see Figure 8 below). This implies that the boundary tangency mechanism can apply only for a values such that $w'(a) > 0$, corresponding to bump death for large a as $-h$ is lowered toward 0 (see Figures 2 and 3). However, as we have noted, $u_2'(0) < 0$ for a sufficiently close to (but above) x_1. Thus, bumps must be born through an internal transition from negativity to positivity (the internal tangency mechanism discussed above) as a increases sufficiently beyond x_1. We summarize the above discussion in the following proposition, stated in terms of loss of existing bumps as a decreases or increases.

PROPOSITION 2.18. *Suppose there exists a_2 such that a bump solution $u_2(x)$ exists, with $u_2(x) > 0$ precisely for $x \in (0, a_2)$. Then as a decreases from a_2, the bump is lost through the internal tangency mechanism. As a increases from a_2, the bump is lost through either the internal tangency mechanism or the boundary tangency mechanism. In the former case, at least one of the internal tangencies must be at $x \neq a/2$.*

Remark 2.19. These birth and death mechanisms suggest that there may exist multibump solutions that satisfy (1.2). The existence and stability of such solutions remain open for future investigation. Note that the existence of multibumps cannot be addressed using (2.1) directly, since multibumps are positive on multiple disjoint regions.

We conclude this subsection by considering a numerical example of bump birth and death. The example coupling function that we introduce here will also be considered in section 3. Define

$$(2.10) \qquad w(x) = (x^2 - c)w_0(x) := (x^2 - c)(De^{-dx^2} - Be^{-bx^2}).$$

We will take $c = 0.5, D = 11, d = 0.05, B = 6$, and $b = 0.035$ as our parameter values unless otherwise stated. This satisfies $(H1)$–$(H5)$; the functions $w_0(x)$ and $w(x)$ for these parameters appear in Figure 5. We also show the corresponding function $W(x) = \int_0^x w(t)\,dt$ on a range of positive x values. Note that in this example, $\lim_{x \to \infty} W(x) > 0$.

For this example, we gradually increase a. We plot $u(a/2)$ versus a in Figure 6, where u satisfies equation (2.2) with h such that equation (2.3) holds. A bump solution is formed when $u(a/2)$ reaches 0, at about $a = a_b \approx 7.14$.
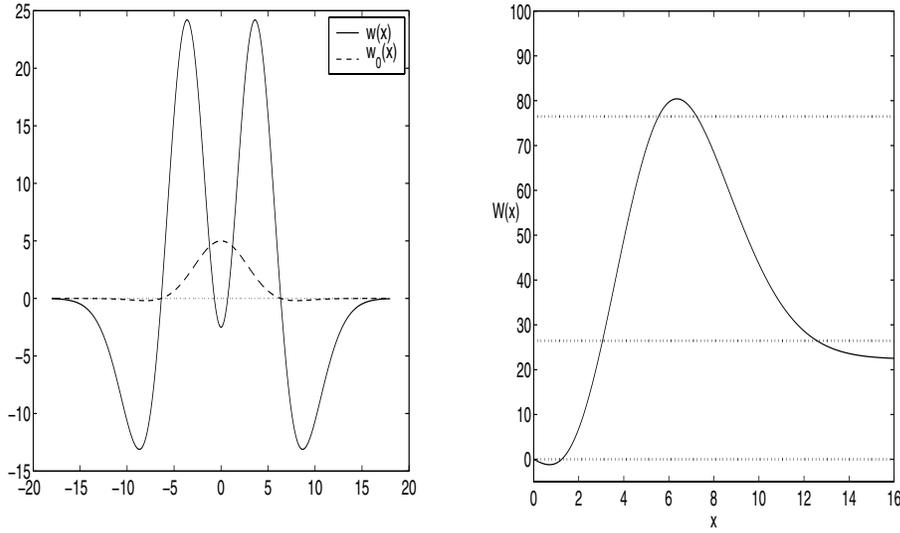
FIG. 5. *Coupling functions from (2.10). The left plot shows $w(x), w_0(x)$ with parameter values as given in the text following (2.10). The right plot shows $W(x)$ for these parameters. The dashed lines correspond to $W(x) = 0$ and to two special values of $-h$ for which bumps exist with spatially inhomogeneous coupling, discussed in section 3.*
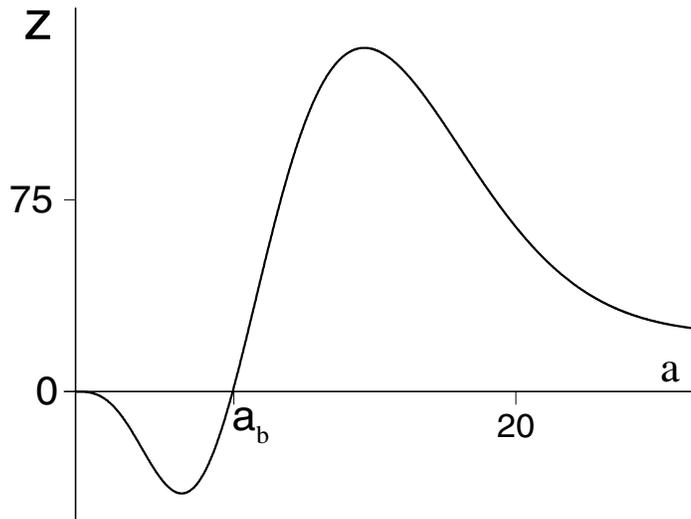

FIG. 6. *The value of u at $a/2$ plotted versus a for $w(x)$ from (2.10). Note that $u(a/2) > 0$ is necessary but not sufficient for bump existence. In this example, a family of bumps is born, as h (and thus a) is varied, as soon as a increases through a_b, such that $u(a/2)$ becomes positive. The bumps must die by a different mechanism, since $u(a/2) > 0$ for all $a > a_b$.*
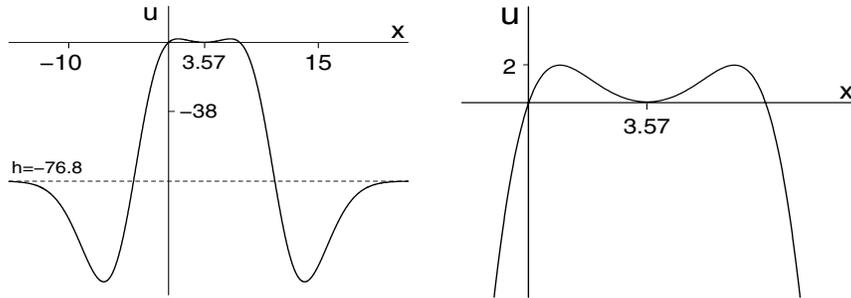
FIG. 7. *Solution $u_2(x)$ at birthpoint $a_b \approx 7.14$ (left), and blowup (right) showing internal tangency of the solution with the x-axis.*

In Figure 7, we plot the solution $u_2(x)$ with $a = a_b$. As a increases from a_b, the bumps that are born persist for an interval of a values; those found for two values of a appear in the top panels of Figure 8. Figure 8 also displays the death of the family of bumps as a continues to increase. At $a = a_d \approx 12.89$, $w(a) = w(0)$ such that $u_2'(0) = u_2'(a) = 0$. For $a > a_d$, bumps cannot exist; careful inspection shows that a representative solution to equations (2.2), (2.3), shown in the lower right plot, goes negative for small $x > 0$ and for x close to, but less than, a. This is not a valid bump solution.

2.5. Linear stability of the bump and bistability. To analyze the linear stability of the bump solution $u_2(x)$, we linearize (1.2) about $u_2(x)$. To compute the correct form of linearized equation, substitute $u = u_2(x) + v(x,t)$ into (1.2). This yields

$$\frac{\partial u}{\partial t} = \frac{\partial v}{\partial t} = -u_2(x) - v(x,t) + \int_{-\infty}^{\infty} w(x-y)H(u_2(y) - v(y,t))\,dy + h.$$

Derivation of the linear equation satisfied to first order by v requires expansion of the Heaviside function H about u_2. The result of this expansion yields [29, 19]

$$(2.11) \quad \begin{aligned} \frac{\partial v}{\partial t} &= -v + \frac{w(x)[v(0,t) - u_2(0)]}{|u_2'(0)|} + \frac{w(x-a_2)[v(a_2,t) - u_2(a_2)]}{|u_2'(a_2)|} \\ &= -v + \frac{w(x)v(0,t)}{u_2'(0)} - \frac{w(x-a_2)v(a_2,t)}{u_2'(a_2)}, \end{aligned}$$

since $u_2(0) = u_2(a_2) = 0$ by construction. Note that if v has its zeros in the same place as those of u, that is, $v(0) = v(a_2) = 0$, then $v' = -v$ and linear stability is immediate.

More generally, for linear stability, we consider perturbations of the form $v(x,t) = e^{\lambda t}v(x)$. Substitution of this expression into (2.11) and cancellation of $e^{\lambda t}$ terms yield the algebraic eigenvalue equation

$$(2.12) \quad (\lambda + 1)v(x) = w(x)v(0)/u_2'(0) - w(x - a_2)v(a_2)/u_2'(a_2).$$

Recall that $u_2'(x) = w(x) - w(x - a_2)$. Thus, (2.12) is equivalent to

$$(2.13) \quad (\lambda + 1)v(x) = \frac{w(x)v(0) + w(x - a_2)v(a_2)}{w(0) - w(a_2)}.$$
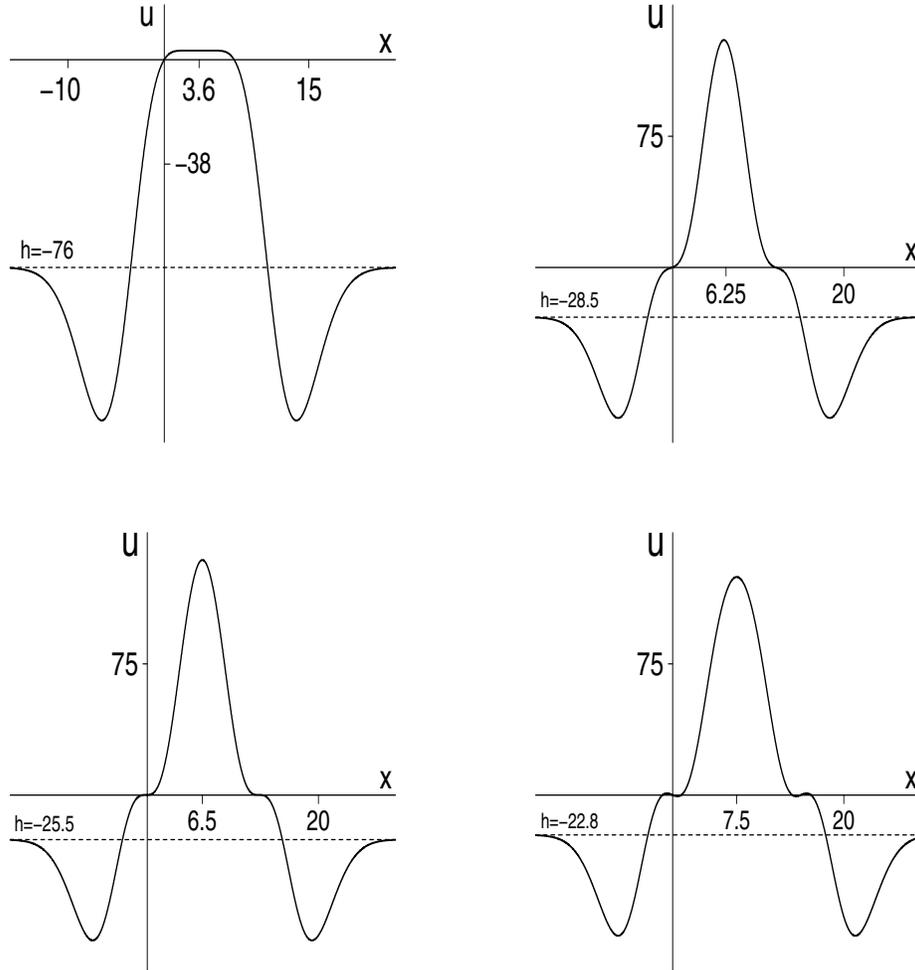
FIG. 8. *Solutions to equations* (2.2), (2.3) *at* $\epsilon = 0$: $a = 7.24$ *(upper left) just after bump birth,* $a = 12$ *(upper right) just before bump death,* $a = 12.89$ *(lower left) where bump death occurs, and* $a = 13$ *(lower right) just after bump death. Note that the solution shown in the lower right is not a valid solution to* (2.1).

Eigenvalues occur at those λ values for which (2.13) has a nontrivial solution $v(x)$. (Note that any such solution decays to 0 asymptotically, since $w(x), w(x - a_2)$ do.) Substitution of $x = 0$ and $x = a_2$ into (2.13) yields a pair of equations in the unknowns $v(0)$ and $v(a_2)$, namely,

$$(2.14) \qquad (\lambda + 1)v(0) = \frac{w(0)v(0) + w(a_2)v(a_2)}{w(0) - w(a_2)},$$

$$(\lambda + 1)v(a_2) = \frac{w(a_2)v(0) + w(0)v(a_2)}{w(0) - w(a_2)}.$$

If $v(a_2) = 0$, then $v(0) = 0$, and only the trivial solution $v \equiv 0$ satisfies (2.13). We

have already observed that perturbations with $v(0) = v(a_2) = 0$ cannot cause an instability, based on (2.11). Thus, assume that $v(a_2) \neq 0$. We use the first equation in (2.14) to write $v(0)$ as a function of $v(a_2)$. Upon substitution of this expression into the second equation in (2.14), cancellation of the nonzero quantity $v(a_2)$ multiplying each term, and algebraic manipulation, we obtain the following quadratic equation in λ:

$$(2.15) \qquad \lambda^2 \left(w(0) - w(a_2)\right)^2 + \lambda \left(\left(w(0) - w(a_2)\right)^2 + w^2(a_2) - w^2(0) \right) = 0.$$

The solution $\lambda = 0$ of (2.15) corresponds to translation invariance of the bump. The other solution of (2.15) satisfies

$$(2.16) \qquad\qquad\qquad \lambda = \frac{2w(a_2)\left(w(0) - w(a_2)\right)}{\left(w(0) - w(a_2)\right)^2}.$$

Recall that $w(a_2) < w(0) < 0$. Thus, the unique solution λ of equation (2.16) is real and negative, and the bump solution is linearly stable.

Note from (1.2) that $u = c := h + \int_{-\infty}^{\infty} w(x)\, dx$ is a stationary, spatially uniform solution, provided that $c > 0$. When this solution exists, the same linearization calculation that yields (2.11) yields the linearized stability equation $dv/dt = -v$, since for small perturbations $c - v > 0$, such that $H(c - v) = 1$. Thus, the spatially uniform state is linearly stable, when it exists, which implies that (1.2) features bistability, at least in terms of linear analysis. This is consistent with the findings of [20], in which a network of bursting thalamic cells with an effectively off-center form of coupling displayed bistability between a spatially localized and a spatially uniform state. In [20], however, the spatially uniform state corresponded to a complete absence of activity.

3. Spatially inhomogeneous coupling. It has been argued that the coupling between cells should be spatially inhomogeneous, reflecting local structural variations [2, 3]. In this section, we use analysis and numerics to consider how such a modification affects properties of bump solutions of (1.2). To this end, we consider bump solutions of the equation

$$(3.1) \qquad\qquad \frac{\partial u(x,t)}{\partial t} = -u(x,t) + \int_{-\infty}^{\infty} w(x-y)p(y)H(u(y,t))\, dy + h.$$

To allow for concrete calculations and numerics, we mostly consider a spatial inhomogeneity used, for example, in [2], namely,

$$(3.2) \qquad\qquad\qquad p(x) = 1 + \epsilon(1 + \cos(\rho x + \phi)).$$

Without loss of generality, we take $\rho = 1$.

In subsection 3.1, we will consider the special case of $\phi = 0$, restricting our attention to bumps on $(0, a)$. In subsection 3.2, we will address the general bump existence question for $p(x)$ given by (3.2). We shall see that, in contrast to the spatially homogeneous case, the presence of inhomogeneity implies that for fixed $p(x)$, for each bump starting point, there is only a small, discrete set of background input levels for which bumps can occur, each with a unique corresponding size. Based on the mechanisms that we observe with $p(x)$ given by (3.2), we expect qualitatively similar results for nonperiodic $p(x) = 1 + \epsilon p_0(x)$ (see Remark 3.4 at the end of the section). Further, at least for the case of $p(x)$ given by (3.2) and $w(x)$ given by (2.10), we find that among the possible bump sizes, there is a certain invariant size selected independent of ϕ and of bump starting position. Possible functional implications of these results are considered in the discussion in section 4.

3.1. Bumps on $(0, a)$ with no phase shift ($\phi = 0$). Note that spatial inhomogeneity in coupling may destroy spatial translation invariance of bump solutions. For clarity, we first consider the special case of bumps on $(0, a)$ with phase shift $\phi = 0$. We will illustrate the key observation that for a fixed spatial pattern of coupling (fixed ρ and ϕ) and a fixed starting point of an activity bump (here $x = 0$), there is only a small, discrete set of possible bump sizes that can be selected. That is, the spatial inhomogeneity induces a form of bump pinning.

As previously, a bump must satisfy $u(0) = u(a) = 0$ and $u(x) > 0$ if and only if $x \in (0, a)$, for some positive number a. If a bump solution $u(x)$ exists for some a, the Heaviside function H in equation (3.1) implies that $u(x)$ must satisfy

$$(3.3) \qquad u(x) = \int_0^a w(x - \eta) p(\eta) \, d\eta + h$$

for that a. Thus, to find a bump solution, we first seek a for which $u(0) = u(a) = 0$, with $u(x)$ specified by (3.3).

The corresponding equations are

$$(3.4) \qquad 0 = \int_0^a w(\eta) p(\eta) \, d\eta + h$$

and

$$(3.5) \qquad 0 = \int_0^a w(a - \eta) p(\eta) \, d\eta + h.$$

Subtracting these two equations, i.e., (3.5)−(3.4), yields

$$(3.6) \qquad g(a) := \int_0^a w(a - \eta) p(\eta) \, d\eta - \int_0^a w(\eta) p(\eta) \, d\eta = 0.$$

To find candidate values of a, we first seek solutions of $g(a) = 0$, given by

$$(3.7) \qquad \int_0^a w(\eta) p(\eta) \, d\eta = \int_0^a w(a - \eta) p(\eta) \, d\eta.$$

Now, from the substitution $y = a - \eta$, note that

$$\int_0^a w(a - \eta) p(\eta) \, d\eta = \int_0^a w(y) p(a - y) \, dy.$$

But $p(a - y) = 1 + \epsilon(1 + \cos(a - y)) = 1 + \epsilon(1 + \cos a \cos y + \sin a \sin y)$. Hence, if $a = 2n\pi$ for any integer n, then $p(a - y) = p(y)$, and we find

$$g(2n\pi) = \int_0^a w(y) p(y) \, dy - \int_0^a w(\eta) p(\eta) \, d\eta = 0.$$

Thus, $a = 2n\pi$ solves $g(a) = 0$ for any integer n (see Figures 9 and 11). However, we also need (3.4), (3.5) to hold such that $u(0) = 0$ and $u(a) = 0$, which occurs only for those special values of n such that $-h = \int_0^{2n\pi} w(\eta) p(\eta) \, d\eta \, (= \int_0^{2n\pi} w(2n\pi - \eta) p(\eta) \, d\eta$ since $g = 0$), which may or may not be positive, as required.

Remark 3.1. This does not imply there is a special biological significance to bump sizes that are even integer multiples of π. If $\rho \neq 1$, then other zeros result here. The point is that the nature of the spatial variation $p(x)$ selects possible bump sizes.
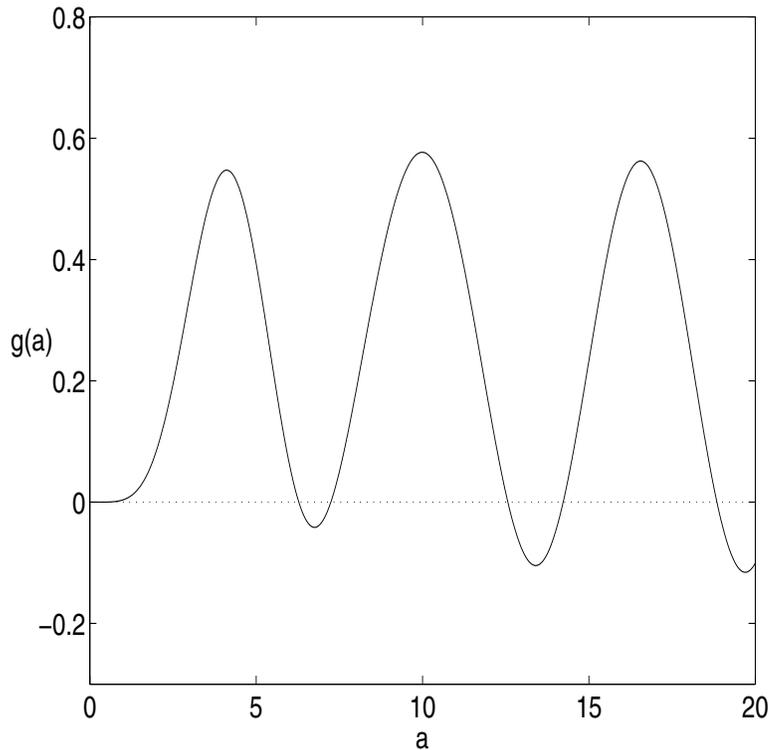
FIG. 9. *The function $g(a)$, defined in (3.6), for $w(x)$ from (2.10) with our usual parameter values. Note that $g(0) = g(2\pi) = g(4\pi) = 0$ and that there are other zeros of g that are not even integer multiples of π.*

There also may be other solutions of $g(a) = 0$. We seek these numerically. To do so, we apply Matlab directly, and we also check our results by using XPPAUT [12] to solve an ordinary differential equation for $g(a)$, derived in the second subsection of the appendix.

We consider now the coupling function $w(x)$ defined in equation (2.10) in the previous section and shown in Figure 5, namely,

$$w(x) = (x^2 - c)w_0(x) := (x^2 - c)(De^{-dx^2} - Be^{-bx^2}),$$

with $c = 0.5, D = 11, d = 0.05, B = 6$, and $b = 0.035$ as usual.

The resulting $g(a)$, for $\epsilon = 0.01$, appears in Figure 9. Numerically, the zeros of $g(a)$ in the set of positive a are $\{2\pi, 7.25, 4\pi, 14.23, 6\pi, \ldots\}$, where the zeros that are not integer multiples of π form a single sequence in which the difference between subsequent elements tends to 2π, since $w(x)$ tends to 0 as $x \to \infty$. We find qualitatively similar results, namely, a countable collection of isolated zeros with similar behavior as $a \to \infty$, for a variety of other parameter sets for $w(x)$ with $\epsilon > 0$.

We note that in general, $g'(0) = g''(0) = g'''(0) = 0$ (see subsection 5.2 of the appendix for a proof). Moreover, we find from (5.8) in the appendix that

$$g^{(4)}(a) = -g''(a) - 3w''(a)p'(a) - 2w'(a)p''(a) + w'''(a)(p(0) - p(a)),$$

so $g^{(4)}(0) = 0$, while

$$g^{(5)}(a) = -g'''(a) - 4w'''(a)p'(a) - 5w''(a)p''(a) - 2w'(a)p'''(a) + w^{(4)}(a)(p(0) - p(a)),$$

so $g^{(5)}(0) = -5w''(0)p''(0) = 5\epsilon w''(0) > 0$. This gives a sense of the behavior of g near $a = 0$, which depends on ϵ.

Since $p(x) = 1 + O(\epsilon)$, it is obvious that the zeros of g do not depend on ϵ. More explicitly, the function $g(a)$ defined in (3.6) can be rewritten as

$$g(a) = \int_0^a w(\eta)p(a - \eta)\,d\eta - \int_0^a w(\eta)p(\eta)\,d\eta.$$

Upon substitution of definition (3.2) for p with $\rho = 1$ and $\phi = 0$ and application of a trigonometric identity for $\cos(a - \eta)$, this yields

$$(3.8) \qquad g(a) = \epsilon \left[(\cos a - 1) \int_0^a w(\eta)\cos(\eta)\,d\eta + \sin a \int_0^a w(\eta)\sin(\eta)\,d\eta \right],$$

which will also be useful below.

Once we have found the zeros of g for a particular choice of parameters (including ϵ), it remains to check whether these really correspond to a values for which (3.4), (3.5) hold, for some $h < 0$. Only in that case will a bump possibly exist. Note that we restrict further to those a values such that

$$(3.9) \qquad \frac{d}{da} \int_0^a w(\eta)p(\eta)d\eta = w(a)p(a) < 0,$$

since only a_2, but not a_1, gives a valid bump in the $\epsilon = 0$ case. In the example shown, the zeros $a \approx 7.25$ and $a = 4\pi$ of g are the only ones which satisfy (3.4), (3.5), and (3.9) for some $h < 0$. The corresponding h values for $\epsilon = 0$ are $h \approx -76.09$ and $h \approx -26.45$, respectively, although these depend on ϵ. The intersections of these values of h with $W(x)$ for $\epsilon = 0$ are displayed in Figure 5. In Figure 10, we plot the corresponding bump solution for $a \approx 7.25$ with $\epsilon = 0.1$. Figure 11 shows the bump solutions for $a = 4\pi$ with $\epsilon = 0, 0.1$, and 0.2, respectively. Note that the bump with $a \approx 7.25$ loses its symmetry for $\epsilon > 0$, while the bump with $a = 4\pi$ is symmetric about $a/2 = 2\pi$ for all ϵ by the 2π-periodicity of $\cos(x)$ and $\sin(x)$. Further, in both cases, the bump widths are independent of ϵ.

3.2. General case: Bumps on (b_1, b_2) with arbitrary ϕ. In this section, we will arrive at the following result: Given a spatial inhomogeneity of coupling of the form (3.2), with ϕ fixed, for any bump starting point b_1, there is a small, discrete set of possible bump sizes. Moreover, there is a subset of these sizes (possibly empty, but nonempty for the main example that we have been considering) which are possible for *all* choices of b_1 and ϕ.

In the general case, the bump existence equations become

$$(3.10) \qquad 0 = \int_{b_1}^{b_2} w(b_2 - \eta)p(\eta)\,d\eta + h$$

and

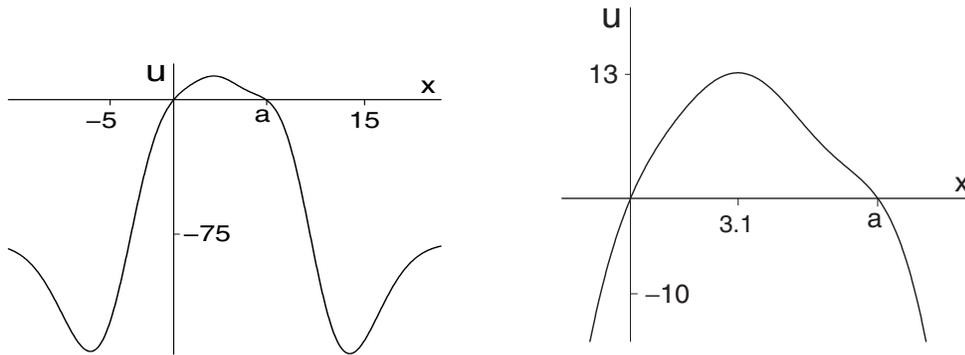$$(3.11) \qquad 0 = \int_{b_1}^{b_2} w(b_1 - \eta)p(\eta)\,d\eta + h,$$

FIG. 10. *Solution at $a \approx 7.25$ and $\epsilon = .1$ (left) and blowup (right). Note that the solution is not symmetric around $x = \frac{a}{2}$ when $\epsilon > 0$ and a is not an even multiple of π.*
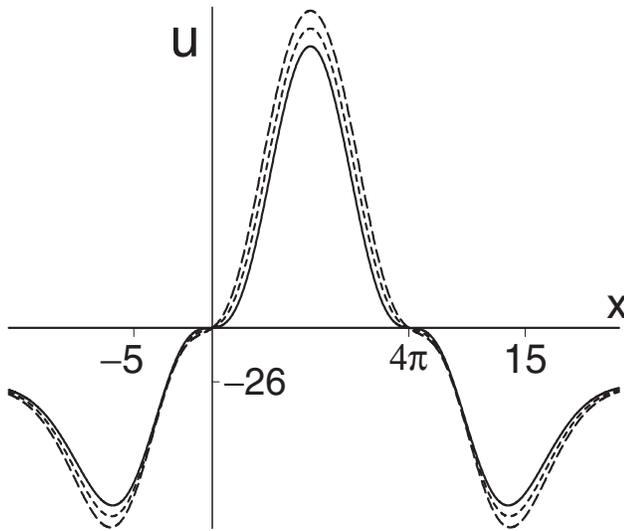

FIG. 11. *Solutions at $a = 4\pi$ and $\epsilon = 0$ (solid curve), $\epsilon = .1$ (dashed curve), and $\epsilon = .2$ (long dashed). Note that solutions are symmetric around $x = \frac{a}{2}$ when $\epsilon > 0$ and a is an even multiple of π.*

where we use (b_1, b_2) to denote the interval on which the bump is positive to avoid confusion with our earlier use of a_1, a_2. Again, we subtract to obtain

$$(3.12) \qquad 0 = \int_{b_1}^{b_2} w(b_2 - \eta)p(\eta)\,d\eta - \int_{b_1}^{b_2} w(b_1 - \eta)p(\eta)\,d\eta.$$

We seek solutions of (3.12), which are exactly the solutions of the following equation, attained by change of variables and by setting $z_i = b_i - \phi$ for $i = 1, 2$:

$$(3.13) \quad 0 = g(z_1, z_2) := \int_0^{z_2 - z_1} w(y)p(b_2 - y)\,dy + \int_0^{z_2 - z_1} w(y)p(b_1 - y)\,dy.$$

It is not apparent by inspection that $g(z_1, z_2)$ as defined in (3.13) is a function of z_1, z_2 only. However, using the definition of p in (3.2) and trigonometric sum and difference
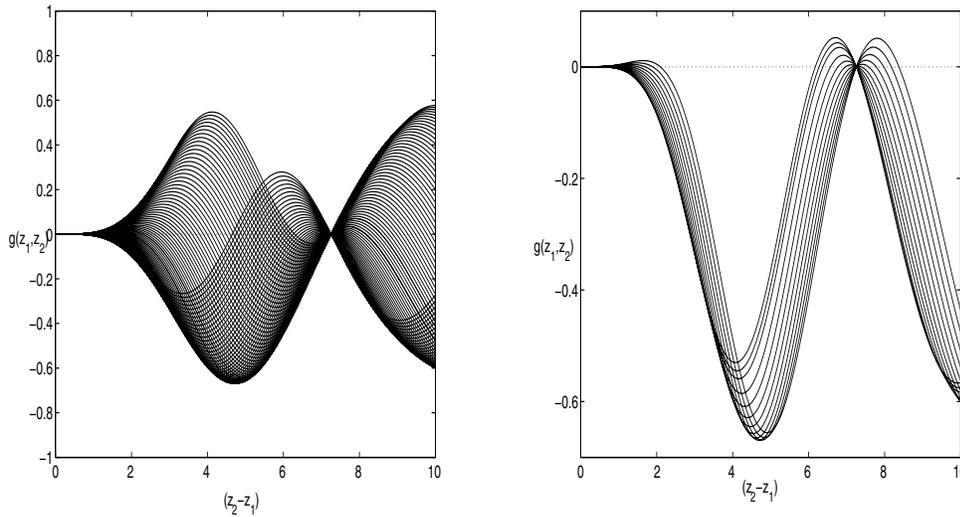
FIG. 12. *The function $g(z_1, z_2)$ given in (3.14). Each single curve in each plot shows $g(z_1, z_2)$ versus $z_2 - z_1$ for fixed z_1. Different curves correspond to different z_1 values. Note that $z_2 - z_1 \approx 7.25$ is a zero of $g(z_1, z_2)$ for all z_1. The right plot shows a closer view around $z_2 - z_1 \approx 7.25$, with fewer curves shown than on the left.*

identities, one can calculate that

$$(3.14) \quad g(z_1, z_2) = \epsilon \int_0^{z_2 - z_1} w(y) \left[\cos y (\cos z_2 - \cos z_1) + \sin y (\sin z_2 + \sin z_1) \right] dy.$$

Note that (3.8) corresponds to a special case of (3.14), with $z_1 = 0$. Further, as noted in subsection 3.1, the zeros of $g(z_1, z_2)$ are independent of $\epsilon > 0$.

Again, the realizable bump sizes, determined by (3.10), (3.11) with the restriction $h < 0$, are a subset of the set of the zeros of g. For fixed ϕ, if we start with $b_1 = \phi$ (that is, $z_1 = 0$), then we recover exactly the bump sizes found with $\phi = 0$. As b_1 is varied from ϕ (or, equivalently, z_1 is varied from 0), then we may pick out different bump sizes. *Some of these, however, may be invariant under changes in z_1.* Indeed, Figure 12 shows plots of $g(z_1, z_2)$ for $w(x)$ from (2.10) and $p(x)$ from (3.2). To produce this figure, z_1 was systematically varied (increasing from 0), and for each fixed z_1, z_2 was varied from z_1 up to $z_1 + 10$ to form an individual curve. The figure shows the resulting $g(z_1, z_2)$ values for each fixed z_1 plotted versus $z_2 - z_1$; that is, each curve has been translated so that it begins at $z_2 - z_1 = 0$, with $g = 0$ correspondingly. The value $z_2 - z_1 = z^* \approx 7.25$ gives a zero of g, corresponding to the existence of a bump solution with $h < 0$, for each starting position z_1. The close-up in the right panel of the figure shows how $\partial g(z_1, z_1 + z^*)/\partial z_2$ passes through 0 as z_1 is varied. Note that similar results were obtained with various other choices of parameter values in $w(x)$.

Remark 3.2. Since the bump size $z_2 - z_1 \approx 7.25$ is realized for all z_1, and since $z_i = b_i - \phi$, this size is invariant under changes in ϕ. That is, for any choice of ϕ and starting position b_1, if $b_2 \approx b_1 + 7.25$, then there is a bump solution $u(x)$ of width approximately equal to 7.25 such that $u(x) > 0$ precisely for $x \in (b_1, b_2)$. Although this solution retains its width, it will occur at different levels of h for different choices of b_1, b_2, ϕ.
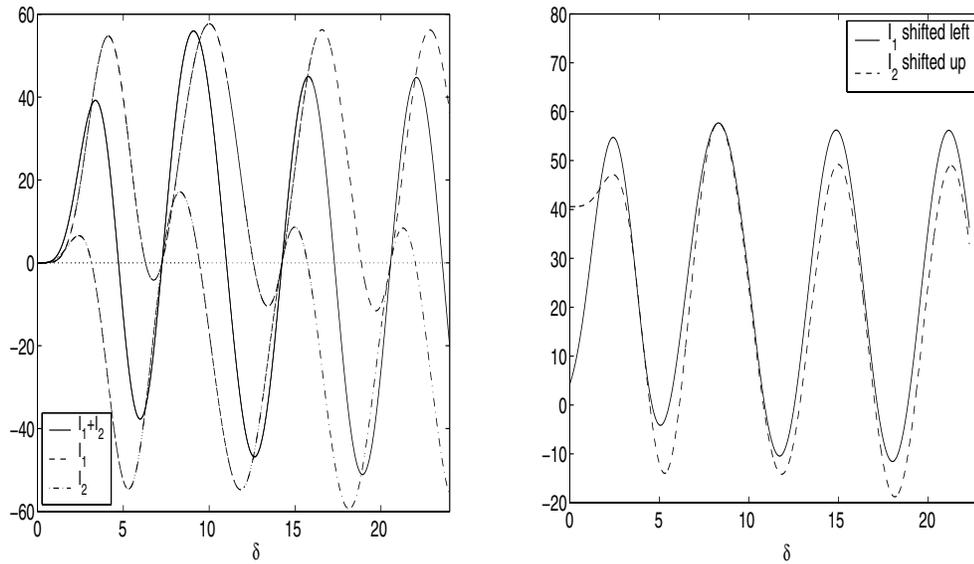
FIG. 13. *Components of* (3.16) *for* $w(x)$ *given in* (2.10) *with usual parameter values. The left plot shows* $I_1(\delta) + I_2(\delta)$ *(middle curve, solid),* $I_1(\delta)$ *(upper curve, dashed), and* $I_2(\delta)$ *(lower curve, dash-dotted), graphed versus* δ. *Note that zeros* δ *of* $I_1(\delta)$ *that are not even multiples of* π, *such as* $\delta \approx 7.25$, *are also zeros of* $I_2(\delta)$. *Since the plot appearance suggests that* $I_1(\delta), I_2(\delta)$ *might be shifted translates of each other, we illustrate graphically in the right plot that this is not the case.*

To understand why there is an invariant bump size, set $\delta = z_2 - z_1$ in (3.14), such that g becomes

$$(3.15) \qquad g(z_1, \delta) = \epsilon \int_0^{\delta} w(y) \left[\cos z_1 \left(\cos y (\cos \delta - 1) + \sin y \sin \delta \right) \right.$$
$$\left. + \sin z_1 \left(\sin y (\cos \delta + 1) - \cos y \sin \delta \right) \right] dy.$$

The function $g(z_1, \delta)$ has some obvious nontrivial zeros, such as $(z_1, \delta) = ((4m + 3)\pi/4, (4n + 1)\pi/2)$ and $(z_1, \delta) = ((4m + 1)\pi/4, (4n + 3)\pi/2)$ for any integers m, n, but these do not give bumps, as they do not solve (3.10), (3.11).

Note that when $z_1 = 0$, the definition of $g(z_1, \delta)$ in (3.15) reduces to (3.8) for $g(a)$ in the $\phi = 0$ case, which for $w(x)$ given by (2.10) with our usual parameter values has a zero at $a = z^* \approx 7.25$. Indeed, we can factor out $\cos z_1$ from the first term on the right-hand side of equation (3.15) and $\sin z_1$ from the second term to write

$$(3.16) \qquad\qquad g(z_1, \delta) = \epsilon(\cos z_1 I_1(\delta) + \sin z_1 I_2(\delta)),$$

where $I_1(\delta) = 0$ for $\delta = 2\pi, z^*, 4\pi, \ldots$. If there are zeros of $I_2(\delta)$ within this set, then these represent potential bump sizes that are independent of starting position and phase (which were encoded in z_1). Numerical experiments suggest that the zeros of $I_1(\delta)$ that are not even multiples of π are also zeros of $I_2(\delta)$; see Figure 13.

Remark 3.3. Although we have not explored what happens with coupling functions $w(x)$ other than that given in (2.10), the form of (3.14), (3.15) strongly suggests that the phenomena observed here do not depend on the exact form of $w(x)$.

Remark 3.4. For general $p(x) = 1 + \epsilon p_0(x)$ with $p_0(x)$ not necessarily periodic, (3.10), (3.11) still apply, with bumps occurring when both are satisfied. One can also

solve (3.12) to find candidate bump endpoints b_1, b_2, with solutions independent of ϵ as above. Thus, we expect that for each fixed $p_0(x)$ and bump starting position b_1, there will be a small number of possible bump sizes selected. We do not know whether or not there will exist an invariant size, independent of starting position, for general $p_0(x)$, however.

4. Discussion. In this paper, we consider localized, stationary activity bump solutions of the rate model (1.1), which describes the evolution of activity in a neuronal population. Following previous work stemming from [1], we take $f(u(y,t)) = H(u(y,t))$, the Heaviside step function, which is an analytically tractable case that has been shown to organize solution structure for some more general forms of f [15]. A key new feature in this paper is that the coupling function $w(x)$ represents off-center coupling. Off-center coupling models the effective pattern of synaptic inputs to an excitatory population in an excitatory-inhibitory (E-I) network with no recurrent excitation, but rather E to I, I to E, and I to I connections.

In this setting, under certain assumptions, we prove that for nonzero h, (1.1) has exactly one time-independent, localized solution satisfying $u(x) > 0$ if and only if $x \in (0, a)$ for a positive, finite constant a. This shows that coupling need not be locally positive to allow for the existence of such a sustained, localized solution. Earlier results showed that the combination of recurrent excitation and long-range inhibition yields the existence of a pair of bump solutions, a linearly stable wider one and an unstable narrower one, to (1.1) [1, 13, 17, 4, 5]. Here we find that for off-center coupling, the unstable bump does not exist, while the single bump that does exist is linearly stable. The nonlinear stability of these bump solutions remains open for investigation.

We show that the range of activity levels h over which bumps can exist, and correspondingly the range of possible bump widths, is finite. Since there is at most a single bump for each h, this brings up the question of how bumps are born and disappear as h varies. We have discussed two types of mechanisms by which this may occur. One mechanism, which can apply to bump birth or death, is the appearance of a point or points inside $(0, a)$ at which u becomes negative. This fits in well with our results showing that a bump can develop an internal local minimum while remaining a valid bump, with $u > 0$ on $(0, a)$. The second mechanism, which can generate only bump death, not bump birth, is a loss of positivity at the edges $x = 0$ and $x = a$ of u. Numerically, we observe bump birth via the former mechanism and bump death via the latter. These mechanisms will not occur when the coupling function $w(x)$ is not off-center (i.e., when there is recurrent excitation). Further, we do not consider temporally dynamic solutions. It is possible that there may be interactions of time-dependent solutions with stationary bumps, which remain to be explored.

We also do not consider temporal details of synaptic dynamics. Our results require sufficiently strong long-range inhibition for bumps to exist with off-center coupling. Thus, our analysis supports the idea that when long-range inhibition is weak [10], slow synaptic dynamics may be necessary to allow for localized activity [20]. Even richer forms of pattern formation can be expected when models incorporating such additional features are considered in future work.

In section 4, we allow for spatial variations in coupling strength, which may correspond to regional structural variations in the brain [2]. Numerically, we observe that this induces bump pinning, such that for each fixed starting position, bumps exist for only a small, discrete set of background input levels h, each with a single corresponding width. Moreover, a unique invariant width is selected, which is possible

at all starting positions. The form of the relevant equations suggests that these results do not depend on the exact form of the coupling function $w(x)$ or on the fact that it is off-center, although this remains to be thoroughly explored. We provide mathematical insight into this size invariance (e.g., Figure 13), but we do not provide analytical proof that this size invariance must occur.

Is it physiologically plausible that spatial inhomogeneities in coupling strength could so severely limit the possible background input levels needed for bumps? We can only speculate on this issue. Since it is believed that attention has significant effects on neuronal activity across wide areas (for example, [11]), it seems possible that the background input level to a brain region could be related to attention. We know from experience that attention is needed to allow for effective working memory or navigation, for example; one needs to first pay attention to a stimulus if one wishes to remember it, and one needs to maintain focus on the memory of this stimulus to keep it "in mind" until it is internalized. Perhaps attention is the process of bringing overall network activity in an appropriate brain region to a level at which a bump can form and subsequently maintaining this level to sustain the localized bump. Since bump sizes are selected by integral conditions relating the spatially homogeneous and inhomogeneous parts of the coupling pattern, perhaps some part of cognitive decline with aging or disease could be associated with a loss of effectiveness of a subset of synaptic connections, which could compromise the "orthogonality" of the system.

Similarly, while a severe limitation on the number of possible bump sizes might initially seem computationally restrictive, there would be advantages to this limitation. In particular, suppose that only a unique bump size were realizable in a certain brain area and that bumps were always symmetric about their centers. If an activity level $u > 0$ were observed from one cell in that area (e.g., by a neuron postsynaptic to it from another area), this would immediately indicate the exact distance of the presynaptic cell from the center of any bump to which it belonged, and activity levels of two cells would suffice to indicate exactly which other cells were in the bump and with which activity levels. This allows for highly efficient decoding by the postsynaptic cell. Note that we observe the development of asymmetric bumps when the coupling is spatially inhomogeneous and the bump length is not an even integer multiple of 2π. Even without symmetry, inputs from a small number of cells in a bump would effectively convey information about the entire bump. Of course, this requires that the postsynaptic cell somehow "knows" that a bump exists in the presynaptic area, and is highly speculative, but nonetheless it suggests that there might be some computational relevance to the bump pinning phenomenon that we have observed.

5. Appendix.

5.1. Coupling profile. The activity levels $u_E(x,t)$ and $u_I(x,t)$ of coupled excitatory and inhibitory populations satisfy the model equations [28, 1, 19]

$$(5.1) \qquad \begin{aligned} \frac{\partial u_E}{\partial t} &= -u_E + w_{EE} * f_E(u_E) - w_{IE} * f_I(u_I) + h_E, \\ \tau \frac{\partial u_I}{\partial t} &= -u_I + w_{EI} * f_E(u_E) - w_{II} * f_I(u_I) + h_I, \end{aligned}$$

where $w * f(u)$ denotes the convolution $\int_{-\infty}^{\infty} w(x-y) f(u(y,t)) \, dy$, $f_i(u)$ is the firing rate function for population i, and w_{ij} denotes the synaptic connection function from population i to population j, which we take here to be nonnegative for all i, j. We consider (1.1) to represent a reduction of (5.1), with $w_{EE} \equiv 0$, to a single equation for the activity level of the excitatory population. The connection function $w(x)$ that we

consider in (1.1), as shown in Figure 1, corresponds to the time-independent input to the excitatory population that results when precisely those excitatory cells at $x = 0$ are active.

To derive the function shown in Figure 1, we therefore set the time derivatives in system (5.1) to zero. This gives $u_E = h_E - w_{IE} * f_I(u_I)$. We assume $h_E > 0$ and aim for an activity profile of u_E which has the form of $w(x)$ shown in Figure 1. This will imply that the activity of cells at $x = 0$ has the desired effect on the activity of the other cells in the excitatory population. For simplicity, assume that $w_{IE}(x)$ has a simple profile; for example, suppose that each inhibitory cell inhibits only those excitatory cells that share its x-coordinate. Then we seek an activity profile of u_I which has the qualitative form of $-w(x)$, for $w(x)$ shown in Figure 1.

Time-independence implies that $u_I = h_I + w_{EI} * f_E(u_E) - w_{II} * f_I(u_I)$. Further, the assumption that only those cells at $x = 0$ are active gives

$$(5.2) \qquad u_I(x) = h_I + w_{EI}(x) - w_{II} * f_I(u_I),$$

although other positive coefficients of w_{EI} may result from non-Heaviside choices of f_E. Thus, the mathematical justification of off-center coupling for (1.1), as in Figure 1, may be achieved by finding a consistent solution of (5.2) having the qualitative form of $-w(x)$, for an appropriate firing rate function f_I. Note that (5.2) has a form very similar to that of the steady state equation (2.1) analyzed in this paper, but with a spatially varying input function, as studied, for example, in [1]. The desired solution would be positive on $(-\infty, -b) \cup (-a, a) \cup (b, \infty)$ for some $b > a > 0$. The proof of the existence of such a solution remains open.

5.2. Derivation of ODE. Recall that for $p(x) = 1 + \epsilon(1 + \cos x)$, we define

$$(5.3) \qquad g(a) = \int_0^a w(a - \eta)p(\eta)\, d\eta - \int_0^a w(\eta)p(\eta)\, d\eta.$$

Thus, using integration by parts, the fact that $w(x)$ is even, and the fact that $w'(0) = 0$, we have

$$(5.4) \qquad \begin{aligned} g'(a) &= p(a)(w(0) - w(a)) + \int_0^a w'(a - \eta)p(\eta)\, d\eta \\ &= w(a)(p(0) - p(a)) + \int_0^a w(a - \eta)p'(\eta)\, d\eta. \end{aligned}$$

Similarly,

$$(5.5) \qquad g''(a) = -w(a)p'(a) + w'(a)(p(0) - p(a)) + \int_0^a w(\eta - a)p''(\eta)\, d\eta$$

and

$$(5.6) \qquad \begin{aligned} g'''(a) = &- 2w'(a)p'(a) - w(a)p''(a) + w''(a)(p(0) - p(a)) + w(a)p''(0) \\ &+ \int_0^a w(\eta - a)p'''(\eta)\, d\eta. \end{aligned}$$

But since

$$p'''(\eta) = -p'(\eta),$$

(5.6) and (5.4) can be combined to give

$$(5.7) \quad g''' + g' = w(a)[p(0) - p(a) + p''(0) - p''(a)] - 2w'(a)p'(a) + w''(a)(p(0) - p(a)).$$

Finally, the fact that

$$p''(x) = -\epsilon \cos x$$

yields $p(x) + p''(x) = 1 + \epsilon$ for any x, such that $p(0) + p''(0) - (p(a) + p''(a)) = 0$. Thus, the ODE (5.7) simplifies to

(5.8) $g''' + g' = -2w'(a)p'(a) + w''(a)(p(0) - p(a)) = \epsilon(2w'(a)\sin a + w''(a)(1 - \cos a))$.

Note that from (5.3), (5.4), (5.5), (5.6), it follows that

$$g(0) = g'(0) = g''(0) = g'''(0) = 0\,.$$

REFERENCES

[1] S. AMARI, *Dynamics of pattern formation in lateral-inhibition type neural fields*, Biol. Cybernet., 27 (1977), pp. 77–87.

[2] P. C. BRESSLOFF, *Travelling fronts and wave propagation failure in an inhomogeneous neural network*, Phys. D, 155 (2001), pp. 83–100.

[3] P. C. BRESSLOFF, *Bloch waves, periodic feature maps, and cortical pattern formation*, Phys. D, 89, (2002), 088101.

[4] C. CHOW AND Y. GUO, *Existence and stability of standing pulses in neural networks* I*: Existence*, SIAM J. Applied Dynamical Systems, submitted.

[5] C. CHOW AND Y. GUO, *Existence and stability of standing pulses in neural networks* II*: Stability*, SIAM J. Applied Dynamical Systems, submitted.

[6] E. P. CHRISTIAN AND F. E. DUDEK, *Electrophysiological evidence from glutamate microapplications for local excitatory circuits in the CA1 area of the rat hippocampus*, J. Neurophysiol., 59 (1988), pp. 110–123.

[7] C. L. COLBY, J. R. DUHAMEL, AND M. E. GOLDBERG, *Oculocentric spatial representation in parietal cortex*, Cereb. Cortex, 5 (1995), pp. 470–481.

[8] A. COMPTE, N. BRUNEL, P. GOLDMAN-RAKIC, AND X.-J. WANG, *Synaptic mechanisms and network dynamics underlying spatial working memory*, Cereb. Cortex, 10 (2000), pp. 910–923.

[9] C. L. COX, J. R. HUGUENARD, AND D. A. PRINCE, *Heterogeneous axonal arborizations of rat thalamic reticular neurons in the ventrobasal nucleus*, J. Comp. Neurol., 366 (1996), pp. 416–430.

[10] C. L. COX, J. R. HUGUENARD, AND D. A. PRINCE, *Nucleus reticularis neurons mediate diverse inhibitory effects in thalamus*, Proc. Nat. Acad. Sci. USA, 94 (1997), pp. 8854–8859.

[11] A. K. ENGEL, P. FRIES, AND W. SINGER, *Dynamic predictions: Oscillations and synchrony in top-down processing*, Nat. Rev. Neurosci., 2 (2001), pp. 704–716.

[12] B. ERMENTROUT, *Simulating, Analyzing, and Animating Dynamical Systems: A Guide to XPPAUT for Researchers and Students*, SIAM, Philadelphia, 2002.

[13] G. B. ERMENTROUT, *Neural nets as spatio-temporal pattern forming systems*, Rep. Prog. Phys., 61 (1998), pp. 353–430.

[14] S. FUNAHASHI, C. J. BRUCE, AND P. S. GOLDMAN-RAKIC, *Mnemonic coding of visual space in the monkey's dorsolateral prefrontal cortex*, J. Neurophysiol., 61 (1989), pp. 331–349.

[15] K. KISHIMOTO AND S. AMARI, *Existence and stability of local excitations in homogeneous neural fields*, J. Math. Biol., 7 (1979), pp. 303–318.

[16] C. R. LAING, W. C. TROY, B. GUTKIN, AND G. B. ERMENTROUT, *Multiple bumps in a neuronal model of working memory*, SIAM J. Appl. Math., 63 (2002), pp. 62–97.

[17] C. R. LAING AND C. C. CHOW, *Stationary bumps in networks of spiking neurons*, Neural Comp., 13 (2001), pp. 1473–1494.

[18] E. K. MILLER, C. A. ERICKSON, AND R. DESIMONE, *Neural mechanisms of visual working memory in prefrontal cortex of the macaque*, J. Neurosci., 16 (1996), pp. 5154–5167.

[19] D. J. PINTO AND G. B. ERMENTROUT, *Spatially structured activity in synaptically coupled neuronal networks:* II. *Lateral inhibition and standing pulses*, SIAM J. Appl. Math, 62 (2001), pp. 226–243.

[20] J. RUBIN, D. TERMAN, AND C. CHOW, *Localized bumps of activity sustained by inhibition in a two-layer thalamic network*, J. Comp. Neurosci., 10 (2001), pp. 313–331.

[21] P. E. SHARP, H. T. BLAIR, AND J. CHO, *The anatomical and computational basis of the rat head-direction cell signal*, Trends in Neurosci., 24 (2001), pp. 289–294.

[22] E. Shink, M. D. Bevan, J. P. Bolam, and Y. Smith, *The subthalamic nucleus and the external pallidum: Two tightly interconnected structures that control the output of the basal ganglia in the monkey*, Neuroscience, 73 (1996), pp. 335–357.

[23] M. Steriade, E. G. Jones, and R. R. Llinás, *Thalamic Oscillations and Signaling*, Wiley, New York, 1990.

[24] J. S. Taube, *Head direction cells recorded in the anterior thalamic nuclei of freely moving rats*, J. Neurosci., 15 (1995), pp. 70–86.

[25] J. S. Taube, *Head direction cells and the neurophysiological basis for a sense of direction*, Prog. Neurobiol., 55 (1998), pp. 225–256.

[26] D. Terman, J. E. Rubin, A. C. Yew, and C. J. Wilson, *Activity patterns in a model for the subthalamopallidal network of the basal ganglia*, J. Neurosci., 22 (2002), pp. 2963–2976.

[27] R. Traub and R. Miles, *Neuronal Networks of the Hippocampus*, Cambridge University Press, Cambridge, UK, 1991.

[28] H. R. Wilson and J. D. Cowan, *A mathematical theory of the functional dynamics of cortical and thalamic nervous tissue*, Kybernetic, 13 (1973), pp. 55–80.

[29] L. Zhang, *Existence and Asymptotic Stability of Traveling Wave Solutions of Neuronal Network Equations*, Ph.D. thesis, The Ohio State University, Columbus, OH, 1999.